J. Geomag. Geoelectr., **37**., 309-327, 1985

Power Line Radiation Observed by the Satellite "OHZORA"

Ichiro TOMIZAWA* and Takeo YOSHINO**

**Sugadaira Space Radiowave Observatory, University of Electro-Communications, Nagano, Japan*
***Department of Applied Electronic Engineering, University of Electro-Communications, Tokyo, Japan*

(Received March 8, 1985)

The magnetic field strength at the fundamental frequencies 50 Hz and 60 Hz, of power line radiation in the topside ionospheric region has been observed by the instrument aboard the satellite "OHZORA" in the global area. The observation has started on June 1, 1984, in order to measure the magnetic field strength of the power line radiation in the topside ionospheric region over the eastern Asia. The observation instrument consists of a loop antenna and a receiving unit, which can receive the fundamental frequencies (50 and 60 Hz) of power line radiation by means of three narrow-bandwidth filters. It is identified that the origin of the background noises of magnetic fields observed at these frequencies is due to the ELF hisses propagating from the outer plasmasphere. By means of the statistical procedure, the background noise field strength at 50 or 60 Hz can be determined in comparison with the strength at 55 Hz. If the magnetic field strength is higher than the level of ambiguity, the corresponding position can be specified as the reasonable position of power line radiation. According to the result of observation, the power line radiation at 60 Hz radiated from the Japan Islands seems to spread over the wide area. The observation results also show that the power line radiation over the eastern China reveals a correlation between the statistically reasonable positions of magnetic field strength at 50 Hz and the possible distribution of power lines on the ground.

1. Introduction

The network of power lines have been extended over the world, and the densities of distribution increase quickly year by year. If electric power were, in an ideal case, transfered without loss through power lines from generators to loads, electromagnetic fields from the power lines can be neglected. Power lines are usually constructed on non-ideal locations such as non-uniform ground and near-by conductors, and they are occasionally connected to unbalance loads. Phase and amplitude unbalances of voltage and current appear on power lines. Induced electromagnetic fields due to the unbalances increase more than the limit of neglection in the vicinity of the power lines. Sometimes, telephone lines or other kinds of signal transmission lines extended along power lines are interfered

from induced currents or voltages due to the electromagnetic fields of power lines. Some energies of the electromagnetic fields are dissipated into the ground and near-by conductors by the ohmic loss, and into the space. An amount of dissipated energies seems to increase even if the rate of dissipation keeps constant since the world total electric generation power is increasing. The amount of electromagnetic energy dissipation has not yet been investigated. To measure the distribution of electromagnetic field strength and to reveal the radiation mechanism are required for this investigation. If the distribution and the mechanism of the power line radiation are revealed, it is possible to predict the world total electromagnetic dissipations in near future. Additionally a method of reduction of electromagnetic fields caused by power lines can be infered by the knowledge of mechanisms of power line radiation.

Authors have been investigating the distribution and the radiation mechanism of the electromagnetic fields from power lines by means of balloons and rockets since 1978 around the Japan Islands (TOMIZAWA and YOSHINO, 1979; YOSHINO and TOMIZAWA, 1981). By the balloon observation, the magnetic field of the power line radiation at 50 and 60 Hz was detected even at the distance of 750 km from the Japan Islands over the Pacific Ocean (TOMIZAWA and YOSHINO, 1979). On the other hand, by the results of the rocket observation, the greater part of the radiated power of electromagnetic fields are reflected downward at the bottom edge of the ionosphere, however, some portion of the radiation fields penetrate upward into the ionosphere (YOSHINO and TOMIZAWA, 1981). It can be thought that electromagnetic fields of the power line radiation from the Japan Islands where power lines are extended are spread over a wide environmental area around the Japan Islands. But these observations covered only a radiation characteristic of power lines over the Pacific Ocean. It is insufficient to describe the distribution characteristics of the electromagnetic field strength in all directions around the Japan Islands, because the inferred radiation mechanism shows the directivity (TOMIZAWA and YOSHINO, 1979). Although the electromagnetic fields are attenuated through the ionosphere, satellite observations give us the distribution of the radiation fields from power lines over the Japan Islands. The satellite observations also give us a global distribution of power line radiation fields. Furthermore, as the satellite observations will be able to elucidate a temporal variation of the fields of power line radiation, it may be possible to estimate the time variation of ELF/VLF emissions induced by the power line harmonic radiations (PARK and MILLER, 1979).

In this paper, an instrumentation, a statistical analysis of observed data, a method of statistical determination of the positions of power line radiation, and preliminaly results over the Japan Islands and the eastern China are discussed.

2. Instrumentation and Observations

An instrument for the satellite observation of power line radiation was designed, taking into consideration of the recent results of the balloon and rocket obser-

vations (TOMIZAWA and YOSHINO, 1979; YOSHINO and TOMIZAWA, 1981). Figure 1 shows the block diagram of the instrument aboard the satellite. The instrument consists of two subsystems: an antenna and a receiver.

The antenna subsystem contains a loop antenna, a pre-amplifier, and an electro-static shield. The loop antenna is made of 100,000 turns of coated copper wire of a diameter of 50 micro-meter wounded on a laminated permalloy core with the dimension of 24 cm × 6 mm × 6 mm. And the size of the electro-static shield of the loop antenna is 25 cm × 4 cm × 4 cm. The output of the loop antenna is terminated by a high-impedance pre-amplifier with a gain of 40 dB. The loop antenna is mounted on the solar side of the satellite body 10 cm apart from the side wall panel. And it is electro-statically shielded by thin aluminum plate. The sensitivities of the loop antenna at 50, 55 and 60 Hz are 35.0, 34.4 and 33.4 V/(A/m), respectively.

The receiver subsystem consists of a programable amplifier, narrow-bandwidth band-pass-filters, amplifiers, detectors, and a calibration oscillator. The gain of the programable amplifier can be changed in three states with a 20 dB step by a real-time command signal from the ground station. Output from the programable amplifier is filtered to select signals at 50, 55 and 60 Hz through three narrow-bandwidth active band-pass-filters. The bandwidth at −3 dB point of the filters is 1 Hz, and the attenuation at 5 Hz apart from the center frequency is more than 40 dB. Those characteristics of the filters are sufficient for selecting spot spectral peaks at the fundamental frequencies of power line radiation. Those filtered signals are amplified (20 dB), and then they are detected by linear detectors with time constants of 1 second. The time constant value is selected in being sufficient for the interval of analog-to-digital (A/D) conversion. The outputs of three detectors and a level-calibration signal are automatically selected for PCM coding in the digital processing unit (DPU) with the interval of 0.125 sec

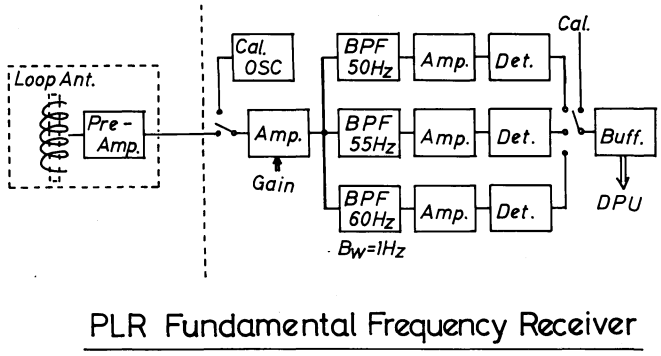

Fig. 1. Block diagram of the instrument aboard the satellite "OHZORA" for measuring magnetic field strength of power line radiation at 50 and 60 Hz. The gain of the amplifier can be changed in four states by a command signal. The band-pass-filter at 55 Hz is used for estimating the background magnetic field strength close to 50 and 60 Hz.

for high bit-rate, and of 0.5 sec for low bit-rate, therefore, those outputs are sampled every 0.5 sec (high bit-rate) and 2.0 sec (low bit-rate), respectively. The function of this subsystem is automatically calibrated by a calibration oscillator. The strength of the magnetic field observed by this instrument is indicated hereinafter in decibel (dB) with respect to the reference magnetic field strength of 1 A/m.

Then an estimation of the field strength above the ionosphere is performed by using the data obtained by the balloons and the rocket. The magnetic field strength at the altitude of 10 km above the Sanriku Balloon Center, Iwate, Japan (39.15°N, 141.82°E) was −110 dB (TOMIZAWA and YOSHINO, 1983). When a theoretical calculation is applied for the above balloon observation data, the magnetic field strength at the bottom of the ionosphere can be obtained as −120 dB. If the magnetic field strength of −120 dB is applied at the bottom of the ionosphere, the magnetic field strength at the altitude of 200 km is estimated as −140 dB by using the attenuation of the rocket observation (YOSHINO and TOMIZAWA, 1981). The estimated strength is comparable to the noise threshold of the instrument. However, as the balloon observation has been performed over the low density area of power lines, the field strength at the altitude of 10 km can be estimated as high as −90 dB above high density areas of power lines. Therefore, the field strength of −120 dB in the topside ionosphere can be observed over high density areas with the margin of 20 dB above the noise threshold level of the instrument. However, more precise disscussion on the penetration of power line radiation must be done by taking into the satellite observation data.

The satellite "OHZORA" was launched on February 14, 1984 into the quasi-polar orbit (inclination 75°, apogee height 865 km, perigee height 354 km, and period 96.9 min). The instrument of power line radiation was turned on June 1, 1984, since then the observations have been made for about 5 months till the end of October, 1984. However, the observations were limited in real-time mode because of electromagnetic interferences from the flux leakage of motors in the data recorder. So the observation data have to be acquired only when the satellite comes into the visible range of the Kagoshima Space Center, Kagoshima, Japan (31.25°N, 131.079°E), and Esrange, Sweden (67.878°N, 21.064°E). After removing interfered portions in observation data in terms of the functional status of the data recorder, the magnetic field strength at three frequencies can be obtained by the correction of frequency responses of the antenna and the receiving subsystems. For the convenience of calculations of the satellite orbital positions, averaging interval of 30 sec has been used in our present analysis. When the magnetic field strength of power line radiation on the satellite is related to the regional distributions of power lines on the ground surface, a statistical determination procedure which will be described in the Sections 4 and 5 is made with correlation to the sub-satellite points on the ground map.

Used were the observation data received at the Kagoshima Space Center from June 1, 1984 to October 25, 1984. Total number of orbits available for investigation of power line radiation was 52 during this period.

3. Origin Determination of Background Magnetic Field at 55 Hz

Observed magnetic field strength at 55 Hz suggests the existence of background noises since the strength is usually from 10 to 15 dB higher than the threshold value of the instrument (−140 dB). This background noise level is comparable to the estimated strength of power line radiation. It is the reason why the statistical procedure is used in this paper to discriminate between power line radiations and background noise.

Two radiation sources can be considered for the origin of the background noises: ELF hisses propagating from the outer plasmasphere (THORNE *et al.*, 1973; TSURUTANI *et al.*, 1975; ONDOH *et al.*, 1983) and atmospherics propagating through the ionosphere.

Occurrence probability of ELF hisses observed at low altitudes is related to local time (TSURUTANI *et al.*, 1975; ONDOH *et al.*, 1983). And occurrence probability of atmospherics also depends on local time (SAO, 1981; KOHTAKI and KATOH, 1982). The magnetic field strength at 55 Hz is plotted with respect to the satellite local time, as shown in Fig. 2. An increase of magnetic field strength during the daytime and a strong day-night asymmetry are found in this figure. There does not usually appear such a strong day-night asymmetry as long as the observation data of the global distribution of atmospherics obtained by KOHTAKI and KATOH (1982). So, thunderstorms seem not to be related to an origin of the magnetic field strength at 55 Hz. Since occurrence probability does show an estimate of probability that field strength exceeds a given threshold value, the occurrence probability agrees well with the variation of the average field strength. Thus, it is considered that the origin of the magnetic field strength observed by OHZORA is ELF hisses which propagate from the outer plasmasphere.

4. Estimations of Hiss Spectral Inclination

It is considered in the previous section that the magnetic field in the frequency range from 50 to 60 Hz is produced principally by ELF hisses. Figure 3 illustrates the amplitude histograms of field strength at 50, 55 and 60 Hz from 31 orbits of observation. This histogram is consisted of 504 points of the observation data of 31 revolutions which covers the wide area of 10–50°N and 100–160°E. The mean values of each field strength are −127.69 Hz), −127.16 dB (55 Hz), and −125.91 dB (60 Hz), and their estimated statistical error of the mean value are 1.21 (50 Hz), 1.18 (55 Hz), and 0.89 dB (60 Hz). The ranges of these statistical ambiguities are indicated by the vertical bars in the left panel of Fig. 4, and the mean values are pointed as the centers of these bars. If spectral inclination between two frequencies is assumed as a difference between mean values of strength at the two frequencies, the spectral inclination between 50 and 55 Hz is 0.53 dB/5 Hz, and that between 55 and 60 Hz is 1.25 dB/5 Hz. These inclinations are indicated by the definite straight lines among the centers of the

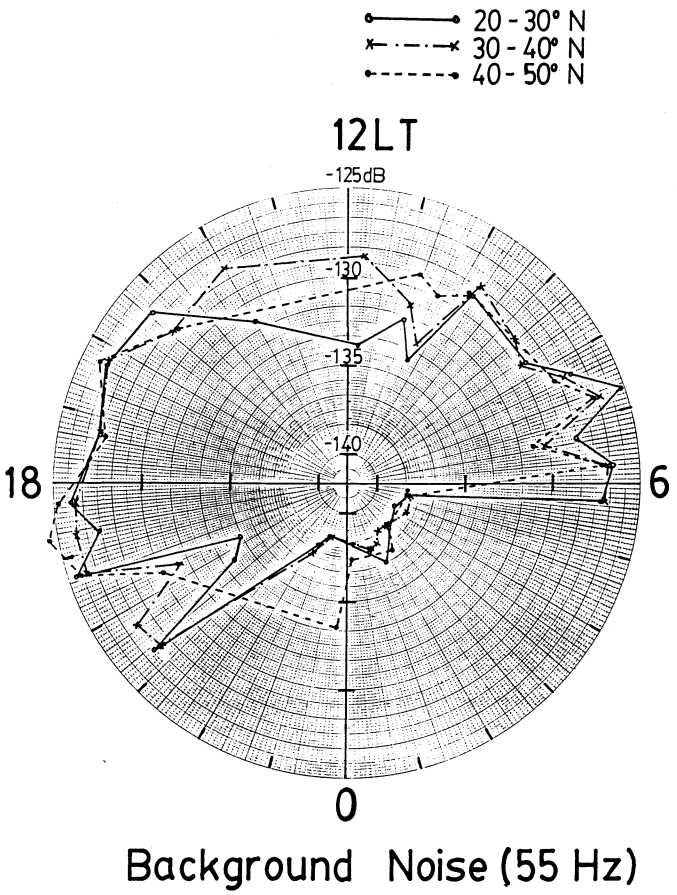

Fig. 2. Polar plot of the magnetic field strength at 55 Hz with respect to the local time. Strength is indicated by a radial distance from the center where the value of strength is −142 dB. The field strength of 0 dB is equal to 1 A/m. The field strength is averaged over these latitude ranges: 20–30°N, 30–40°N, and 40–50°N.

bars. As illustrated in the left panel of Fig. 4, the field strength increases on the average with increasing frequency. This tendency coincide with the characteristics of the ELF hisses observed by OGO-6 (TSURUTANI *et al.*, 1975) if the spectral inclination below 100 Hz is extrapolated from Fig. 3 of TSURUTANI *et al.* (1975) which can be illustrated in the right panel of Fig. 4.

The spectral inclination is also obtained by a cross-correlation method. The magnetic field strength at 50, 55 and 60 Hz must be correlated with each other, because their magnetic field strengths mainly contain field strength of ELF hisses which have broad-band spectral characteristics as illustrated in the right panel of Fig. 4. In other words, if ELF hiss is observed at 50, 55 and 60 Hz, field

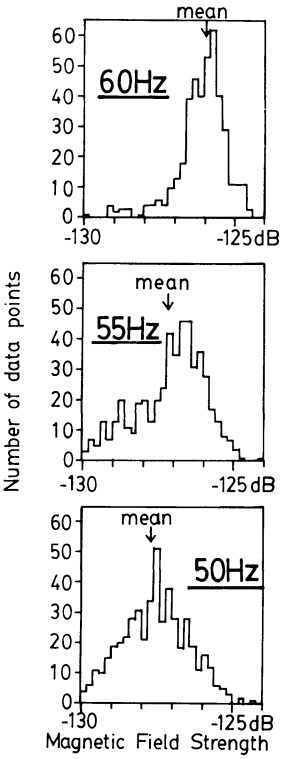

Fig. 3. Amplitude distributions of magnetic field strength at 50, 55 and 60 Hz. 504 observation data are plotted. Mean values of the field strength are −127.69 dB (50 Hz), −127.16 dB (55 Hz), and −125.91 dB (60 Hz), and their correspondent standard deviations are 1.21 dB (50 Hz), 1.18 dB (55 Hz), and 0.89 dB (60 Hz).

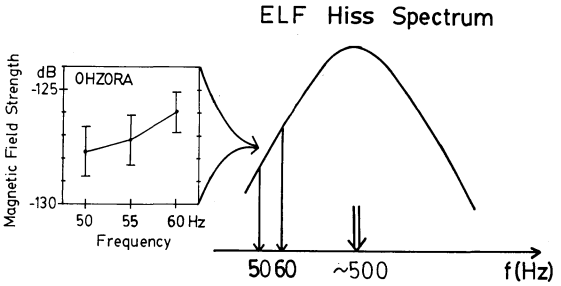

Fig. 4. An ELF hiss spectrum is illustrated in the right panel, according to the observations of THORNE *et al.* (1973) and TSURUTANI *et al.* (1975). Note that the spectral inclination below 100 Hz is extrapolated from Fig. 3 in TSURUTANI *et al.* (1975). The left panel shows the spectrum from 50 to 60 Hz obtained by OHZORA, which indicates the increase of the strength with frequency. The vertical bar at each frequency shows the ranges of these standard deviations, and the solid contour indicating the spectral inclination is drawn in terms of the results of Fig. 3.

strengths at these frequencies must be simultaneously increased. Therefore, the occurrences of increases of field strengths at these frequencies have one-to-one correspondence among them, however, the values of field strength at the three frequencies are different because of the spectral inclination of ELF hisses. If we assume that the differences in the strength among them are equivalent to the spectral inclinations, the correlation function of field strengths at 50 and 55 Hz, or 55 and 60 Hz can be described by a linear equation as following equation,

$$y = x + a, \tag{1}$$

where (a) y is the field strength at 55 Hz, x is the field strength at 50 Hz, and a is the spectral inclination for the frequency range from 50 to 55 Hz; (b) y is the field strength at 60 Hz, x is the field strength at 55 Hz, and a is the spectral inclination for the frequency range from 55 to 60 Hz. Correlation plots of the observation data between 50 and 55 Hz, and between 55 and 60 Hz are shown in Fig. 5(a) and 5(b), respectively. By means of a least-squares method, the values of spectral inclination a are obtained as follows; for the 50–55 Hz correlation in Fig. 5(a) is

$$a = 0.525 \text{ dB/5 Hz},$$

and for the 55–60 Hz correlation in Fig. 5(b) is

$$a = 1.250 \text{ dB/5 Hz}.$$

These values of the spectral inclinations a equal to the values obtained above from the calculations in terms of the mean values.

To clear the coincidence between these two methods, the average of the squared residual of the Eq. (1) at each point to obtain the least value are able to calculate in the following equation,

$$s^2 = (1/N) \sum_{i=1}^{N} (y_i - x_i - a)^2. \tag{2}$$

If the Equation (2) takes a minimum, the first derivative of Eq. (2) with respect to a equals to zero;

$$(-2/N) \sum_{i=1}^{N} (y_i - x_i - a) = 0. \tag{3}$$

Therefore,

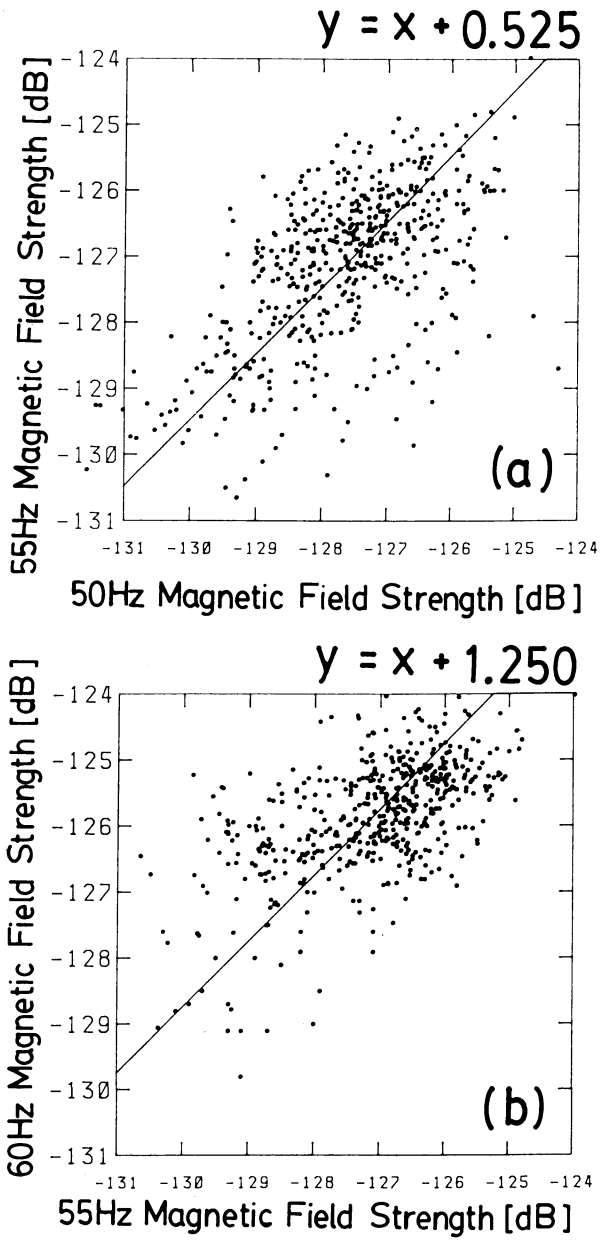

Fig. 5. (a) Magnetic field strength at 50 and 55 Hz is plotted at each observation point. The straight line is drawn by a least-squares method for fitting $y=x+a$; where y is the field strength at 55 Hz, x is the field strength at 50 Hz, and a is a constant value of ELF hiss spectral inclination. The value of the constant a is 0.525 dB, and the average field strength at 55 Hz is 0.525 dB higher than that at 50 Hz. (b) Same format as for (a) except that the frequencies are 55 and 60 Hz. The value of the constant a of the straight line is 1.25 dB, and the average field strength at 60 Hz is 1.25 dB higher than that at 55 Hz.

$$a = (1/N) \sum_{i=1}^{N} y_i - (1/N) \sum_{i=1}^{N} x_i. \tag{4}$$

The right side of Eq. (4) is equal to the mean values of the field strength at 50 and 55 Hz or at 55 and 60 Hz. These mean values have been obtained as shown in the Fig. 3. Thus, the spectral inclinations are calculated from the Eq. (4) using the mean values at each frequency. The assumption on the calculation of the spectral inclinations is able to be obtained by using the mean values which just coincides with the least-squares method. It is the reason why the spectral inclinations obtained by means of the different methods coincide each other. Root-mean-squared (RMS) fitting errors of Eq. (1) to the real observation data are obtained by calculating the Eq. (2). The RMS fitting errors are calculated as 1.09 dB for the frequency range from 50 to 55 Hz, and 0.98 dB for the range from 55 to 60 Hz. It can be implimented that these fitting errors are the ambiguities of the output of the Eq. (1) to calculate magnetic field strength of the background noise at 50 or 60 Hz as compared with the value at 55 Hz.

5. A Statistical Method for Determination of Reasonable Values of Power Line Radiation

As magnetic field strength at 55 Hz indicates the background noise field strength, a method of estimation of values of background noise field strength at 50 and 60 Hz is expressed by the following equations;

$$H_{50}(\text{noise}) = H_{55} - 0.525 \ [\text{dB}], \tag{5}$$

$$H_{60}(\text{noise}) = H_{55} + 1.25 \ [\text{dB}], \tag{6}$$

where H_{50}(noise) and H_{60}(noise) are the estimated background noise field strength at 50 and 60 Hz, respectively, and H_{55} the observed background noise field strength at 55 Hz. These estimated values include some statistical ambiguities determined as 1.09 dB for 50 Hz and 0.98 dB for 60 Hz from the calculation of the RMS fitting errors of the least-squares method described in the Section 4 of this paper.

If an observed value at 50 or 60 Hz is below the level of ambiguity (estimated noise strength plus statistical ambiguity value), it can be considered that the observed magnetic field at 50 or 60 Hz is principally consisted of the magnetic field of ELF hisses. If values of the observed magnetic field strength at 50 or 60 Hz are higher than the level of ambiguity, it can be considered that the observed magnetic field strength has a possibility of origin of power line radiation. This criterion of power line radiation is going to be used in this paper. Therefore, the values, which are higher than the summation of the estimated strength of background noise at 50 or 60 Hz and the statistical ambiguity, are only taken into consideration of the origin of power line radiation. However, the estimation of possibility of power line radiation contains the statistical errors that the

background noise field is considered as the origin of power line radiation. Provided that the background noise is statistically ergodic and gaussian, the probability of misjudgment of the background noise as power line radiation is less than 15.87 percent of the total data points. When all observed data are the background noise, the probability of misjudgment is 15.87 percent of the total observed data. However, as the data observed by OHZORA probably contain the field strength of the origin of power line radiation, the probability of misjudgment will be reduced. If the statistical characteristics of the background and the power line radiation are determined precisely, the accurate probability of misjudgment can also be determined.

6. Observation Results over the Japan Islands

In Fig. 6(a), the satellite "OHZORA" trajectory of the revolution number

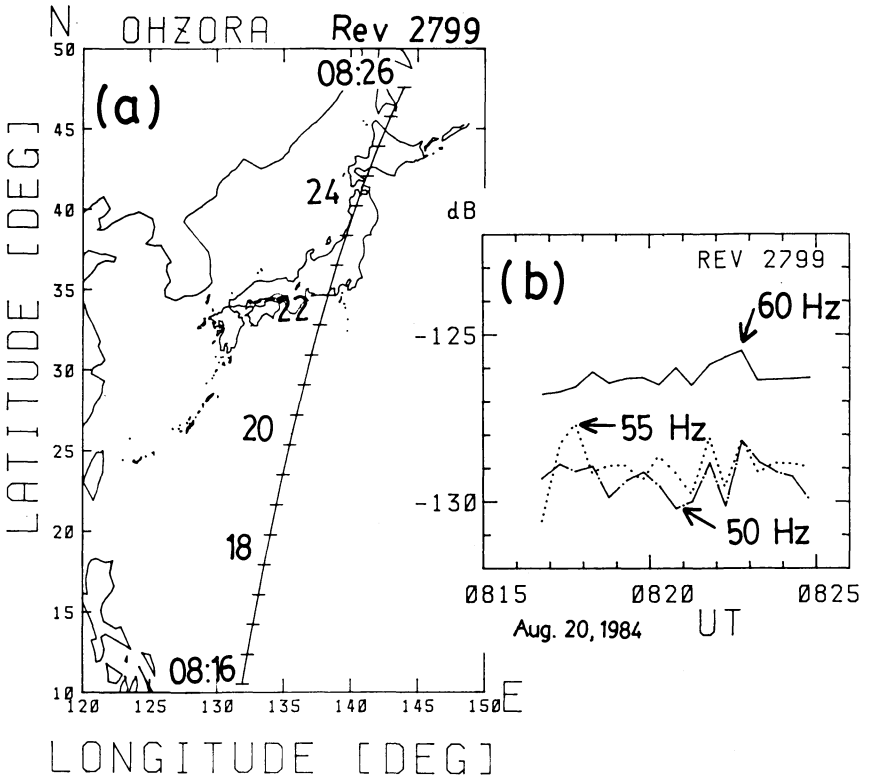

Fig. 6. (a) The subsatellite trajectory and (b) the magnetic field strength at 50, 55 and 60 Hz observed on August 20, 1984. OHZORA passed over the Japan Islands from south to north. The ordinate in (b) is the magnetic field strength in dB with respect to 1 A/m. The magnetic field strength at 60 Hz was the highest field strength of the three frequencies throughout this observation. The strength at 50 Hz was comparable with that at 55 Hz.

of 2799 is projected on the map around the Japan Islands. OHZORA passed over the eastern part of the Japan Islands from south to north. The power line radiation was measured from 08h17m to 08h25m UT on August 20, 1984. And the magnetic field strength observed on this path is shown in Fig. 6(b). The field strength at 60 Hz is approximately 2 dB higher than the field strength at 50 and 55 Hz, and the field strength at 50 Hz is comparable to the strength at 55 Hz. However, the field strength in Fig. 6(b) does not indicate the real field strength of the power line radiation, because the field strength is superposed by ELF hisses.

To apply the procedure described in the Section 5, the field strength of estimated background noise at 50 and 60 Hz is calculated by means of the Eq. (5) and (6). The observed magnetic field strength at 50 and 60 Hz is plotted by solid lines in Figs. 7(b) and 7(c) with respect to the satellite latitude. The magnetic field strength of estimated background noises is also plotted by dashed lines.

The observed magnetic field strength at 50 Hz does not exceed the level of ambiguity which is calculated by adding the estimated background noise level and the statistical ambiguity, while the observed magnetic field strength at 60 Hz exceeds the level of ambiguity almost during the entire observation time, as indicated by the black-painted area in Fig. 7(c). It is therefore considered according to the criterion of power line radiation that (1) no possible position of power line radiation at 50 Hz is observed during this period, and (2) power line radiation at 60 Hz is observed almost during this period. The detected positions as power line radiation at 60 Hz indicated by the black-painted areas in Fig. 7(c) is also indicated by rectangles attached on the left side of the satellite trajectory in Fig. 7(a). The reasonable positions of the power line radiation at 60 Hz do not correspond to the time when OHZORA has passed over the Japan Islands where the density of power line distribution is high. Additionally the reasonable positions at 60 Hz does not terminate at the border of power line frequencies from 60 Hz to 50 Hz as indicated by the dashed line in Fig. 7(a). Therefore, the reasonable positions are not directly related to the power line distribution on the ground. This nonrelationship can be interpreted in two ways; (1) the magnetic field at 60 Hz, which is radiated from the power lines on the Japan Islands, spreads over the wide area, and (2) the background noise field is misjudged as the origin of power line radiation. However, the observed magnetic field strengths at 60 Hz exceed approximately 2 dB with respect to the estimated background from 30 to 35°N as shown in Fig. 7(c). The excess of 2 dB is approximately two times greater than the ambiguity of the estimation of the background noise level at 60 Hz. The possibility of misjudgment of the background noise as the origin of power line radiation is approximately 2.28 percent of the total data points. Thus, it seems that the observed magnetic field at 60 Hz is originated from the power lines on the Japan Islands. If this is true, the magnetic field strength at 50 Hz is 2 to 4 dB less than that at 60 Hz from 30 to 35°N as shown in Fig. 7(b) and 7(c).

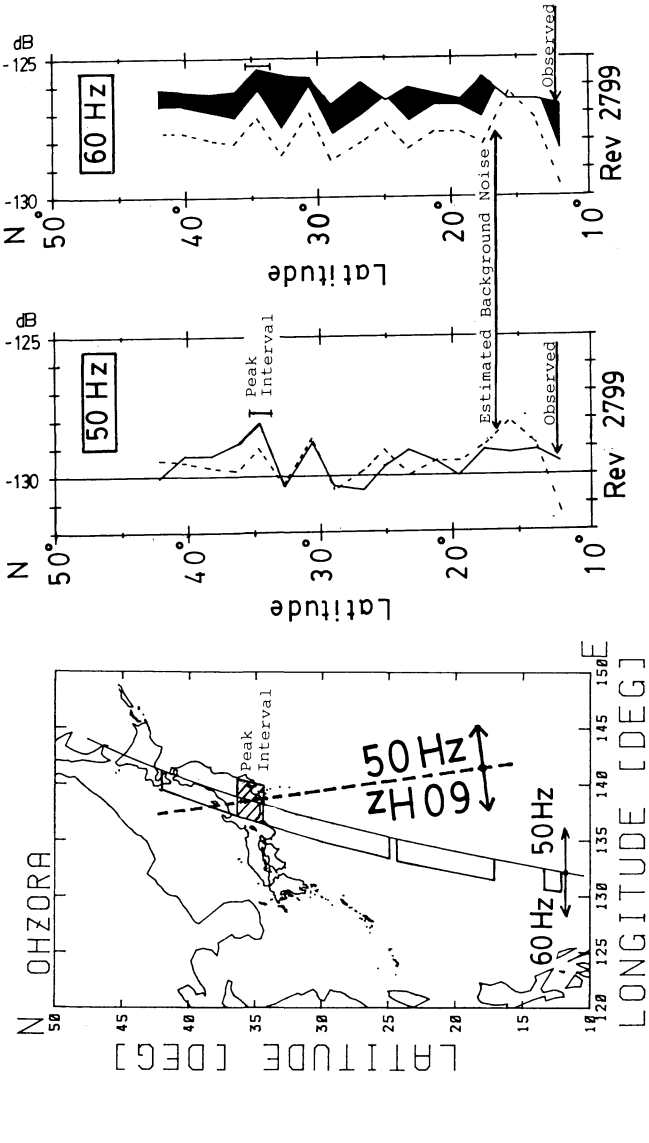

Fig. 7. (a) The reasonable positions of power line radiation are indicated by rectangles along the satellite trajectory. The positions are deduced by Fig. 7(b) and 7(c), and the positions of the peak strength for 50 and 60 Hz are indicated by hatched rectangles. It should be noted that the Japan Islands are divided into two regions of the different frequencies of the commercial power system, as indicated by the dashed line. 50 Hz is occupied in the right side of this dashed line, and 60 Hz in the left side. (b) Magnetic field strength at 50 Hz is plotted against the satellite latitude by a solid line, accompanying the deduced field strength of the background noise at 50 Hz indicated by a dashed line. The observed value of the field strength does not exceed 1.1 dB more than the value of the estimated field strength of the background noise. The 30-second interval of peak strength in the observed values is indicated on the right side of the peak. The position of the peak strength is correspondent to the hatched rectangles on the right side of the satellite trajectory in Fig. 7(a). (c) The format of this figure is the same as in Fig. 7(b). The position of exceeding the deduced noise field strength by 1.0 dB is indicated by a black-painted area. The exceeding positions appear throughout this observation and they are indicated by rectangles on the left side of the trajectory. The 30-second interval of peak strength is also indicated on the right side. The position of the peak strength is indicated by the hatched rectangle on the left side of the trajectory in Fig. 7(a).

It is interesting to note that the positions of the peaks of the magnetic field strength at 50 and 60 Hz are found to appear in correlating with the time of the satellite passing over the Japan Islands. They are indicated by hatched rectangles on the left for 60 Hz and the right for 50 Hz as shown in Fig. 7(a). And the hatched rectangles in the Fig. 7(a) can directly correspond to the positions of the high density of power lines. These results show the good correspondence between the peaks of the field strength and the ground power lines. However, this correspondence can occur by chance. More measurements over the Japan Islands should be continued for further investigation.

7. Power Line Radiation over the Eastern China

Power line radiation is also observed over the eastern part of China by thirteen orbits of the observations as listed in Table 1.

The commercial power line systems in China uses the frequency of 50 Hz, so the investigation is performed only on the magnetic field strength at 50 Hz. Thirteen revolutions of observation data are processed by means of the analyzing process described in the Section 5. The results of the above process are plotted in Fig. 8. The estimated values of the field strength of the background noise are indicated by dashed lines. When the observed magnetic field strength is 1.1 dB higher than the estimated field strength of the background noise, the area higher than the level of ambiguity is painted out with black as shown in Fig. 8. It is interesting that most of painted positions appear in the latitude range greater than 25°N.

Then, the painted positions are correspondent to the satellite positions on the map as indicated in Fig. 9 by hatched rectangles on the satellite trajectories. It is important to note that most of the hatched rectangles are concentrated into

Table 1. Observations over the eastern China.

REV	Date YY/MM/DD	UT HH:MM:SS-HH:MM:SS	Longitude/Latitude East/North (deg.)	Height (km)	Day/ Night
1617	84/06/01	00:55:00-01:03:30	119-133/27-55	726-826	Day
2584	84/08/05	22:47:30-22:53:30	119-126/42-20	380-427	Day
2637	84/08/09	11:35:30-11:43:30	116-126/17-47	561-454	Day
2711	84/08/14	10:42:00-10:47:30	116-122/21-41	500-433	Day
3451	84/10/03	01:03:30-01:08:00	116-122/25-41	438-504	Day
3650	84/10/16	09:30:30-09:40:00	109-118/42-10	821-739	Day
3658	84/10/16	21:48:30-21:59:00	121-135/15-52	515-684	Day
3679	84/10/18	08:05:00-08:17:30	119-133/51-09	829-720	Day
3688	84/10/18	22:07:00-22:13:00	117-127/33-53	614-708	Day
3694	84/10/19	08:13:30-08:24:30	118-129/45-08	819-710	Day
3709	84/10/20	08:20:30-08:31:00	113-124/45-09	814-705	Day
3762	84/10/23	21:01:00-21:10:30	115-129/22-54	612-753	Day
3768	84/10/24	07:10:00-07:22:00	118-130/47-07	803-658	Day

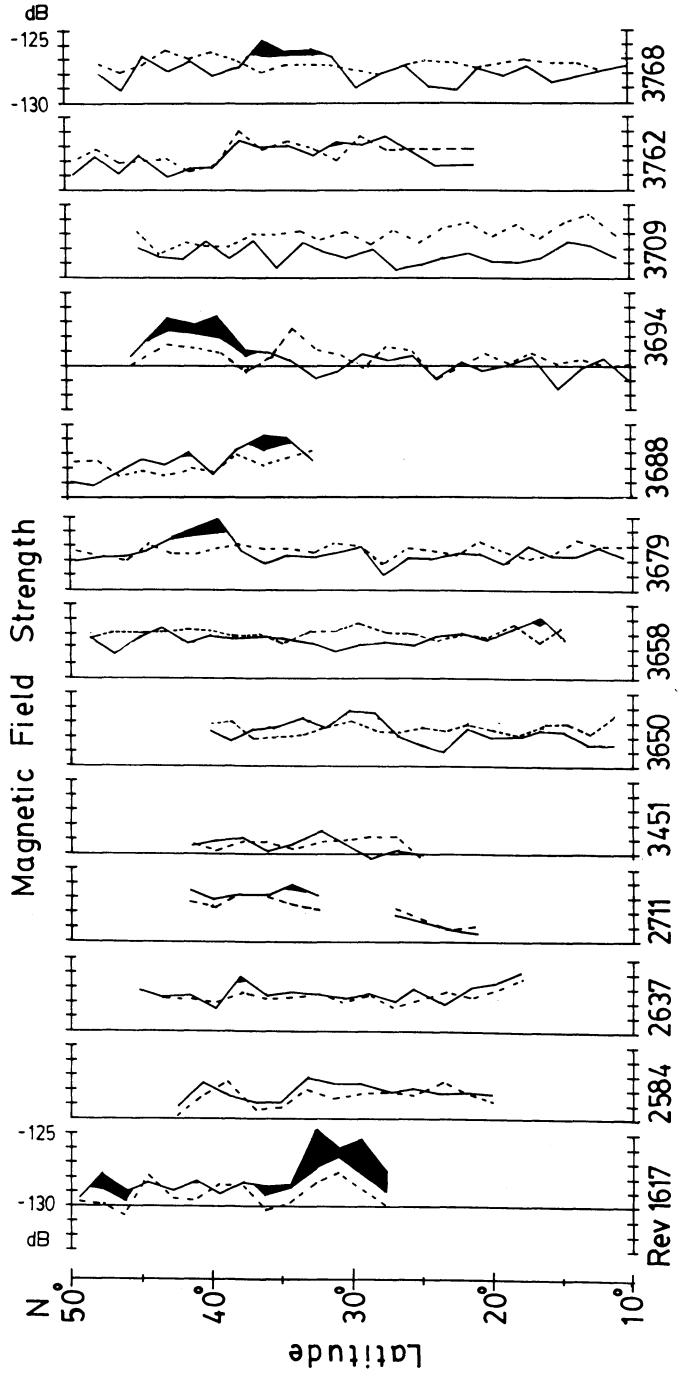

Fig. 8. Observation data of thirteen orbits when the satellite passed over the eastern part of China. Magnetic field strength at 50 Hz of each observation is drawn by the solid line against the latitude of the subsatellite point. Deduced noise value of magnetic field strength at 50 Hz is drawn by a dashed line. The positions where the observed field strength indicated by the solid lines exceed by 1.1 dB more than the deduced noise field strength indicated by the dashed lines, are indicated by black-painted areas.

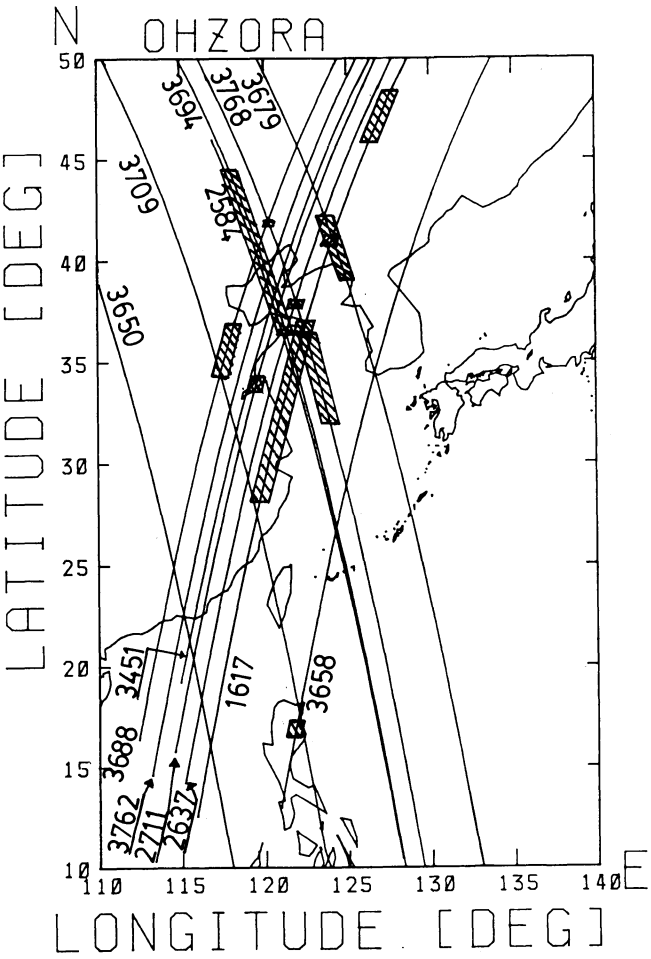

Fig. 9. The positions of exceeding 1.1 dB with respect to the deduced noise field strength indicated by black-painted areas in Fig. 8 are indicated by hatched rectangles attached to each satellite trajectory on the map. The revolution numbers are indicated besides the trajectories. Most of these exceeding positions are concentrated into the region over the eastern China.

the area which is limited in the latitude of 25–45°N and the longitude of 115–125°E. The eastern China has relatively high power consumption area including Shanghai and Peking. The total generated electric power in China of the year 1982 was 3.3×10^{10} kWh, while that in Japan of the year 1982 was 5.8×10^{10} kWh (SOUMU-CHOU TOUKEI-KYOKU, 1984). Therefore, the total generated electric power in China is approximately half of that in Japan. However, the most electric energy in China is generated by the water power which is different from that in Japan where the most electric energy is generated by the steam

power and the atomic power. Generally the length of power line is tend to be long in the case of the water power generation compared to the case of the steam and the atomic power generations. The length of power lines is the most effective to the radiation of the electromagnetic field (TOMIZAWA and YOSHINO, 1979). Hence it can be inferred that the efficiency of radiation from the power lines in China is higher than that in Japan. Additionally, most of the electric energy in China may be generated in the area of the eastern China, which can be deduced from the distribution of the industrial areas in China (CHUU-GOKU SOU-RAN HEN-SHUU I-IN-KAI, 1979). In fact, the statistically reasonable positions of power line radiation do not appear over the western China where the amount of the electric power generation is little compared with the eastern China, and over the sea area where no power line is extended, as seen from Fig. 9.

8. Conclusion

Observations of the magnetic field of power line radiation by the satellite "OHZORA" have started on June 1, 1984. The receiving frequencies of the instrument are 50, 55 and 60 Hz and the bandwidth of the receiver is 1 Hz. The frequencies of 50 and 60 Hz are the fundamental frequencies of commercial power line systems. Magnetic field strength at 55 Hz is used as the reference strength of the background noise level of magnetic field. The observations are limited in the real-time mode because of the interference of the leakage flux of the motor installed in the data recorder aboard the satellite. The real-time mode observation data of power line radiation over the Kagoshima Space Center are used for our present analysis.

The origin of the background magnetic field at 55 Hz is investigated with respect to the local time, based on the data obtained from 52 orbits of real-time mode observations, since the two sources of the origin are closely related to local time. The local time dependency of the magnetic field strength at 55 Hz appears a strong day-night asymmetry and is enhanced in daytime. In addition, the variation of field strength with local time in Fig. 2 is quite similar to the temporal variation of occurrence rate of ELF hisses obtained by the satellite OGO-6 (Fig. 3 of TSURUTANI *et al.*, 1975). The thunderstorm activity does not appear such a night-time decrease and it is sometimes enhanced in nighttime (SAO, 1981; KOHTAKI *et al.*, 1981; KOHTAKI and KATOH, 1982). From these observation results, the origin of the background magnetic field at 55 Hz is considered to be ELF hisses propagating from the outer plasmasphere.

If the background noise at 50, 55 and 60 Hz is due to ELF hisses, its spectral characteristic is required to know for the estimation of background magnetic field strength at 50 and 60 Hz in comparison with the strength at 55 Hz. In fact, the ELF hisses indicate a spectral peak around 500 Hz in the right panel of Fig. 4 (OGO-6 observations), and the magnetic field strength decreases with decreasing frequency from 200 to 100 Hz (Fig. 3 of TSURUTANI *et al.*, 1975). Therefore, there is no estimation of the spectral characteristic of the ELF hisses

from 50 to 60 Hz except for our analysis using the observation data obtained by the satellite "OHZORA". These observation data were obtained at the Kagoshima Space Center. The covering area of these observations is 10–50°N and 100–150°E. The statistical Equations of (5) and (6) are resulted from the data obtained by 31 observations described in Fig. 4. And their RMS fitting errors are also estimated as 1.09 dB for Eq. (5) and 0.98 dB for (6). Statistically the estimated values of the background noise field include the above ambiguities; i.e., 1.09 dB for 50 Hz and 0.98 dB for 60 Hz. Thus, if the observed magnetic field strength at 50 or 60 Hz is higher than the level of ambiguity (estimated background noise level plus ambiguity), the observed strength at 50 or 60 Hz can be considered as to mainly contain a component of the magnetic field of the power line radiation. However, this statistical procedure can produce the possible positions of power line radiation even if the observed strength mainly contains the background noise. The possibility of misjudgment is less than 15.87 percent of the observed data points. Therefore, it must be required to detect the relationship between distribution of possible positions of power line radiation and distribution of power lines on the ground. If these possible positions are produced as the result of misjudgment, the distribution of these position will be randomly spread over a wide area. The detailed estimation of the possibility of misjudgment will be done in terms of more observation data in future.

By the above statistical criterion, the real-time observation data over the Japan Islands and over the eastern China have been analyzed with correlation to the reasonable regions of the power line radiation along the sub-satellite trajectories on the earth, as follows;

(1) The observation data which was obtained by OHZORA over the Japan Islands passing from south to north is applied to investigate for correlating the statistically reasonable regions of power line radiation. The magnetic field strength at 50 Hz does not exceed the values of criterion during this observation, but the strength at 60 Hz exceeds the values of criterion more than half of this observation period. Correlation between the reasonable positions of the power line radiation at 60 Hz and the sub-satellite trajectory on the grid of the earth as shown in the Fig. 7 seems not to be so good because the reasonable positions appear both over the Pacific Ocean of no power line region and over the Japan Islands with high density of power lines. However, on the statistical basis, the observed magnetic field at 60 Hz seems to be radiated from the Japan Islands and the field of power line radiations spreads over a wide area. It is interesting to note that the positions of the magnetic field strength peak at 50 or 60 Hz seem to correspond to the high density areas of power lines in Japan. More observations over the Japan Islands should be required to investigate these relationships.

(2) Observations on the thirteen orbits of the satellite "OHZORA" are used to investigate the power line radiation over the eastern China. The fundamental frequency of Chinese power line system is 50 Hz. The reasonable positions of the magnetic field strength of power line radiation at this frequency

are indicated by the black-painted areas in Fig. 8. In Fig. 9, these reasonable positions are indicated by the hatched rectangles on the sub-satellite trajectories, and most of the hatched rectangles appear over the eastern China. Because these observations were expanded over more wider area as indicated by the satellite trajectories in this figure, the concentration of the reasonable positions of the power line radiation over the eastern China must be meaningful. Thus, it is concluded that the power line radiation over the eastern China is observed by OHZORA.

The authors are greatly indebted to the participants in the "EXOS-C (OHZORA)" satellite project, particularly to Dr. T. Itoh, Inst. Space Astronaut. Sci., who have managed this project, and to Dr. H. Oya, Tohoku Univ., who have managed the payload instruments. Also the authors offer sincere thanks to S. Yamakawa and N. Hiura, University of Electro-Communications, for their help in data analyses. This observation was fully supported by the Institute of Space and Astronautical Science. A portion of data processing was performed in the Data Processing Center, University of Electro-Communications.

REFERENCES

CHUU-GOKU SOU-RAN HEN-SHUU I-IN-KAI, *Chuu-goku Sou-ran, 1980*, p. 299, Ka-zan-dou, Tokyo, 1979.

KOHTAKI, M., I. KURIKI, C. KATOH, and H. SUGIUCHI, Global Distribution of Thunderstorm Activity Observed with ISS-b, *J. Radio Res. Lab.*, **28**, 49–71, 1981.

KOHTAKI, M. and C. KATOH, Global distribution of atmospheric radio noise derived from the global distribution of lightning activity, *Denpa-kenkyuu-sho Kihou, Radio Res. Lab., Japan*, **28**, 411–433, 1982.

ONDOH, T., T. NAKAMURA, S. WATANABE, K. AIKYO, and T. MURAKAMI, Plasmaspheric hiss observed in the topside ionosphere at mid- and low-latitudes, *Planet. Space Sci.*, **31**, 411–422, 1983.

PARK, C. G. and T. R. MILLER, Sunday decreases in magnetospheric VLF wave activity, *J. Geophys. Res.*, **83**, 943–950, 1979.

SAO, K., *Kuu-den*, pp. 91–114, Sei-zan-dou, Tokyo, 1981.

SOU-MU-CHOUU TOU-KEI-KYOKU, *Dai 32 Kai Koku-sai Tou-kei You-ran, 1984*, p. 125, Sou-mu-chou Tou-kei-kyoku, Tokyo, 1984.

THORNE, R. M., E. J. SMITH, R. K. BURTON, and R. E. HOLZER, Plasmaspheric hiss, *J. Geophys. Res.*, **78**, 1581–1596, 1973.

TOMIZAWA, I. and T. YOSHINO, Study of power line radiation I: Balloon observation, *Rep. Univ. Electro-Comm.*, **30**, 101–108, 1979.

TOMIZAWA, I. and T. YOSHINO, Nihon-Rettou Kinbou no Den-ryoku-sen Housya Denjikai Kyoudo, in *Proc. Dai-kikyuu Symposium, Inst. Space Astronaut. Sci., Tokyo*, pp. 100–109, 1983.

TSURUTANI, B. T., E. J. SMITH, and R. M. THORNE, Electromagnetic hiss and relativistic electron losses in the inner zone, *J. Geophys. Res.*, **80**, 600–607, 1975.

YOSHINO, T. and I. TOMIZAWA, Rocket and balloon observations of power line radiation over Japanese Islands, in *Proc. 4th EMC Meeting, Zurich*, 525–530, 1981.